STUDIES ON AN EPITHELIAL (GLAND) CELL JUNCTION

I. Modifications of Surface Membrane Permeability

WERNER R. LOEWENSTEIN and YOSHINOBU KANNO

From the Department of Physiology, Columbia University, College of Physicians and Surgeons, New York

ABSTRACT

Membrane permeability of an epithelial cell junction (*Drosophila* salivary gland) was examined with intracellular microelectrodes and with fluorescent tracers. In contrast to the non-junctional cell membrane surface, which has a low permeability to ions (10^{-4} mho/cm^2), the junctional membrane surface is highly permeable. In fact, it introduces no substantial restriction to ion flow beyond that in the cytoplasm; the resistance through a chain of cells (150 Ω cm) is only slightly greater than in extruded cytoplasm (100 Ω cm). The diffusion resistance along the intercellular space to the exterior, on the other hand, is very high. Here, there exists an ion barrier of, at least, 10^4 Ω cm^2. As a result, small ions and fluorescein move rather freely from one cell to the next, but do not leak appreciably through the intercellular space to the exterior. The organ here, rather than the single cell, appears to be the unit of ion environment. The possible underlying structural aspects are discussed.

INTRODUCTION

When cells enter associations, they often attach themselves intimately at their contact surfaces. Since Bizzozero (1870), a wide variety of attachment forms have become known. They include *desmosomes*, *terminal bars*, and *septate attachments* (see 13, 56, 62, and 75 for a review). Under the electron microscope, the attachments are seen as regions of cell contact at which the cell membranes are closely apposed and sometimes associated with special intracellular (4, 10, 13, 14, 19, 20, 23–25, 27, 30, 32, 39, 42–48, 50–53, 57, 59–61, 63, 68) and extracellular structures (13, 63). The apposition is particularly close in the case of *terminal bars* and *septate attachments* at which the external components of the contact membranes appear to merge (10) or to interconnect (75). Little is known about the functional aspects of these membrane specializations. Earlier work dealt exclusively with the mechanical function of cell adhesion (*cf.* 62). Only recently have studies been carried out on permeability properties of cell attachments (4, 9–11, 32, 33, 41). These studies were concerned with the attachments as a permeability barrier between the cell exterior and the intercellular space. The possible significance of cell attachments in intercellular permeability has not yet been explored. For example, one would like to know whether the permeability properties at the attachment level are the same as those at the rest of the cell membrane; and, in general, whether the over-all diffusion resistance at the confronting surfaces of neighboring cells is similar to that at the surfaces in direct contact with the cell exterior.

The general conception of the cell membrane as a diffusion barrier is that its resistance is uniformly high over all faces of a given cell. The idea derives chiefly from electrophysiological work with blood and gamete cells, and large nerve and

striated muscle fibers. These are, however, a rather special group of cells. The two former are normally unconnected; and the latter are rather loosely associated, have generally wide intercellular spaces, and except for special synaptic contact regions (25, 55, 55 *a*, 68 *a*) and neuroglia contacts (19, 39, 55) have no close cell attachments. This is evident even at the coarse mechanical level. Large nerve and muscle fibers are readily teased apart—a routine practice among neurophysiologists—and continue to function in isolation. It is another matter to attempt to separate cells with attachments. For instance, cells of squamous (epidermis) (6) and cylindrical epithelia (salivary gland cells, see below) are so strongly bonded that, when the attempt is made to pull them apart, they invariably rupture, and their surface membranes remain adhered at their attachments. Also functionally, the nerve and muscle fibers constitute a rather special group which has adapted to transmit electrical signals without appreciable cross-talk between cell neighbors. This obviously requires an uninterrupted barrier for ion diffusion along the cell surfaces; and, indeed, in these elements, except for certain synaptic (1 *a*, 5, 15, 15 *a*, 21, 22, 64, 69–71, 74) and neuroglia contacts (34), the surface resistance in the unexcited state is, in general, high and, within the limits of resolution of the methods, distributed rather uniformly over all cell surfaces (see, for example, 7, 17, 31).

The question raised above is, then, essentially this: Does the attachment affect diffusion from cell to cell? This question is asked here for the case of an association of cylindrical epithelial cells, that of salivary gland cells of *Drosophila flavorepleta* larvae. These cells have attachments of the septate type. The approach consists of driving a current of ions from the interior of one cell to the interior of an adjacent cell, and seeing how much of the current leaks through their contact membranes. It will be shown that the membrane resistance across the contact surface of the cell of the epithelium is so low compared to that of the outer cell surfaces that movement of ions from one cell to the next must be relatively unrestricted. The present paper deals with the electrical measurements and fluorescent tracer studies. Preliminary accounts of these have already appeared (29, 29 *a*). The second paper of this series deals with the pertinent morphological aspects (73).

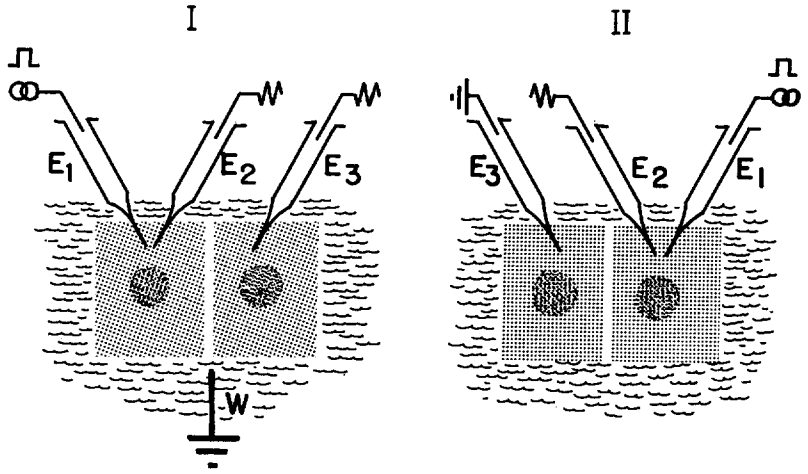

FIGURE 1 Diagram of set-up for electrical measurements. Explanations in the text.

MATERIALS AND METHODS

Salivary gland cells of *Drosophila flavorepleta* larvae were used throughout the work. The larvae were in the early or midstages of the third instar period of development. During this period the gland cells approach their largest size, have distinct boundaries, and do not divide. All experiments were done at room temperature ranging from 20 to 24°C.

ELECTRICAL MEASUREMENTS: The glands were isolated and mounted in a bath of Shen's solution for micromanipulation under a compound or a stereomicroscope. Three micropipettes of the Ling-Gerard (35) type, filled with 3 M KCl, were inserted into cells and connected in two alternative electrode arrangements (Fig. 1). In arrangement *II*, resistance across the contact surface is measured.

Micropipette E_1 serves to pass pulses of current across the contact membrane; E_2, to record the resulting voltage drop across these membranes; and E_3, as a ground electrode in common between the recording and current-passing circuits. In arrangement *I*, a large Ag-AgCl electrode (*W*) serves as common ground lead, and both E_2 and E_3 record membrane voltages. In this arrangement, attenuation of membrane voltage along a series of cells is measured.

In either arrangement, the current was supplied by a square pulse generator and monitored on one of the beams of an oscilloscope. Voltages were displayed on the second oscilloscope beam. They were fed into a d-c amplifier across an electrometer input stage with a negative-capacity feedback, to compensate for electrode impedance and for stray capacities in the recording system. The grid currents were below 10^{-13} amps.

The general procedure was first to use electrode arrangement *I*, then *II*, and then *I* again. In *I*, the penetration of the cells by the micropipettes was accompanied by the appearance of pulses of membrane voltage of characteristic magnitude. This provided a reliable check, aside from visual observation, that the pipettes were in their desired intracellular position. It provided also two convenient indices of the state of the preparation: in measuring resting potential and membrane impedance across the cell surface membranes, one is supplied with two sensitive means for detecting membrane injury.

The micropipettes in arrangement *I*, and E_1 and E_2 in *II*, had tip diameters below 0.5 μ, resistances of 10 to 20 Meg Ω, and tip junction potentials in Shen's solution of less than 2.5 mv. (For further details, see an earlier paper, 36.) E_3 in *II* had somewhat larger diameter, and resistance of 1 Meg Ω or less. Each micropipette was driven by a micromanipulator equipped with an advance mechanism operating in the direction of the pipette axis. This minimized the size of membrane perforations. The cell membrane seemed to seal well around the pipette tip. There were no signs of current leakage upon single, and often even after repeated insertions. Pipette insertions and all related manipulations were done under direct microscopic observation. In good preparations, the cells remained free of opacity and the cell membrane potential and impedance were rather constant for 1 to 2 hours after isolation of the gland. Preparations which developed opacities or showed declines in resting potential of more than 10 per cent in the course of an experiment, or deviated by more than 20 per cent from the normal resting membrane potential and impedance values, were discarded. All experiments were done within ½ hour after gland isolation.

FLUORESCEIN INJECTIONS: For fluorescein injections, we used micropipettes of 5 to 7 μ tip diameter filled with a fluorescein-Na (Uranin, Fisher Scientific Co., New York) solution, 10 mM fluorescein-Na in Shen's solution. The micropipettes were connected to a piston. The preparation was placed across a beam of ultraviolet and observed in the dark field of a compound microscope. With the aid of a simple mirror switch, the preparation could be viewed alternately in ultraviolet and in ordinary light without changing the microscope optics.

CELL SEPARATIONS: The experiments of cell separation referred to in the Introduction were done with microneedles and tweezers driven by a set of three micromanipulators.

PHYSIOLOGICAL SOLUTIONS: Shen's solution (58) modified to the following composition was used: NaCl, 147 mM; KCl, 5.6 mM; $CaCl_2$, 2.25 mM; 5 mM sodium phosphate buffer, pH 7.0.

TERMINOLOGY: The following terms will be used to denote regions of the cell membrane. *Contact membrane*: the region at the cell junction at which close ionic coupling exists. *Luminal membrane*: the region at the lumen which is eliminated as an ion leak by insulating the duct, as, for instance, in the experiment of Fig. 5. *Cell surface membrane*: the rest of the cell membrane.

These are functional terms. As so often when attempts are made at relating functional with structural aspects, the subdivisions here of the cell membrane are somewhat arbitrary, and structural limits are not rigorously definable. In the subsequent paper of this series (73), similar terms are used in a structural sense, and are, therefore, not necessarily coterminous. As to the choice of names, the term "basal membrane" would perhaps have been more appropriate for what we called the "cell surface membrane." We decided not to use this term, to avoid confusion with the basement membrane.

RESULTS

Electrical Measurements

Salivary gland cells of *Drosophila flavorepleta* larvae offer an unusually favorable material for electrophysiological work on contact membranes. The cells are large, have little adventitious tissue, and are quite transparent. Typical dimensions of a good-sized cell are: 80 μ, along the length axis of the gland; 150 μ, along the gland circumference; and 100 μ, in the direction base-to-lumen. The cells are arranged in a single layer of roughly uniform depth. Their outlines, including those of the contact surfaces, are clearly seen in the living cell in phase contrast or in a dark field. The cells are readily impaled with microelectrodes, and it is possible to follow in some detail the progress of the electrodes through the cell interior (Fig. 2).

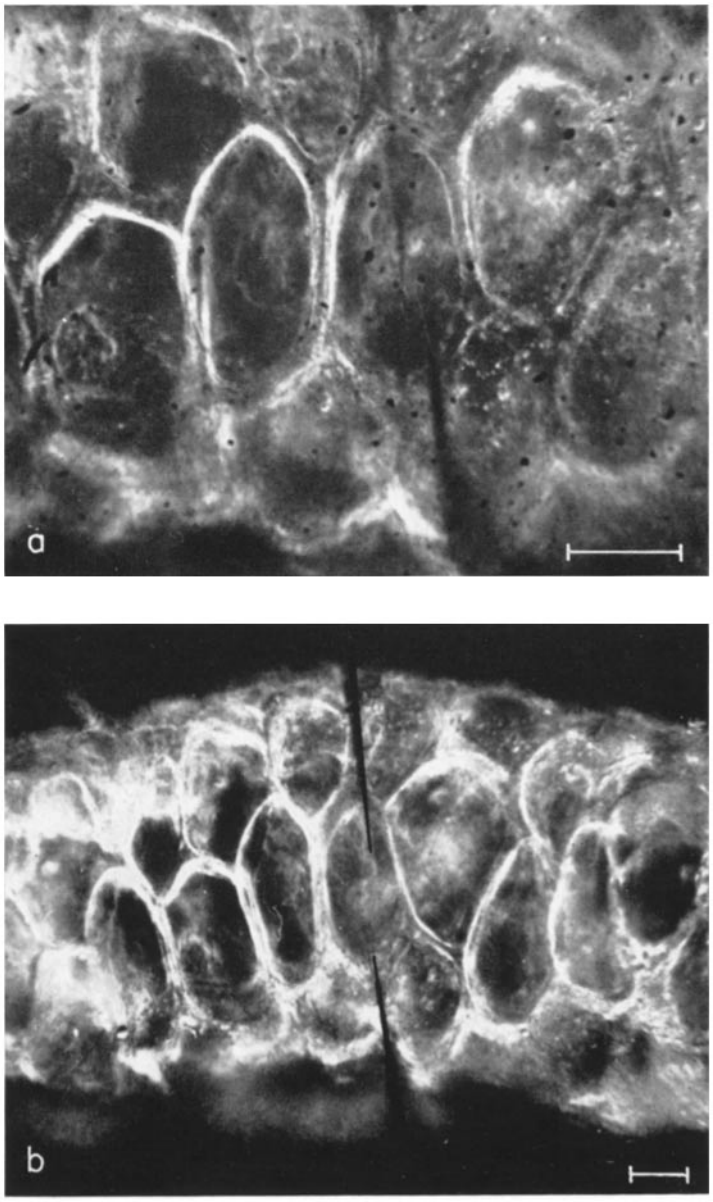

FIGURE 2 Photomicrographs (dark field) of a living, unstained gland. The tips of two micropipettes (retouched in *b* to enhance contrast) are seen in one cell. Calibration, 50 μ.

Since there are no overlapping cellular extensions beyond a zone of 1 μ along the contact contours (73), one can be certain about the position of the electrode tip within a given cell.

INTERCELLULAR COUPLING: Fig. 3 illustrates the results of an experiment in which square pulses of current of varying intensity are passed between the extracellular fluid and a microelectrode located in one cell (*A*); and the resulting changes in membrane potential are recorded across the cell surface membranes with electrodes placed inside this cell and in a contiguous one. The changes of potential for any given current value are nearly the same in the two cells. The slope of the potential change *vs.* total input current, which for outward currents amounts to 5 to

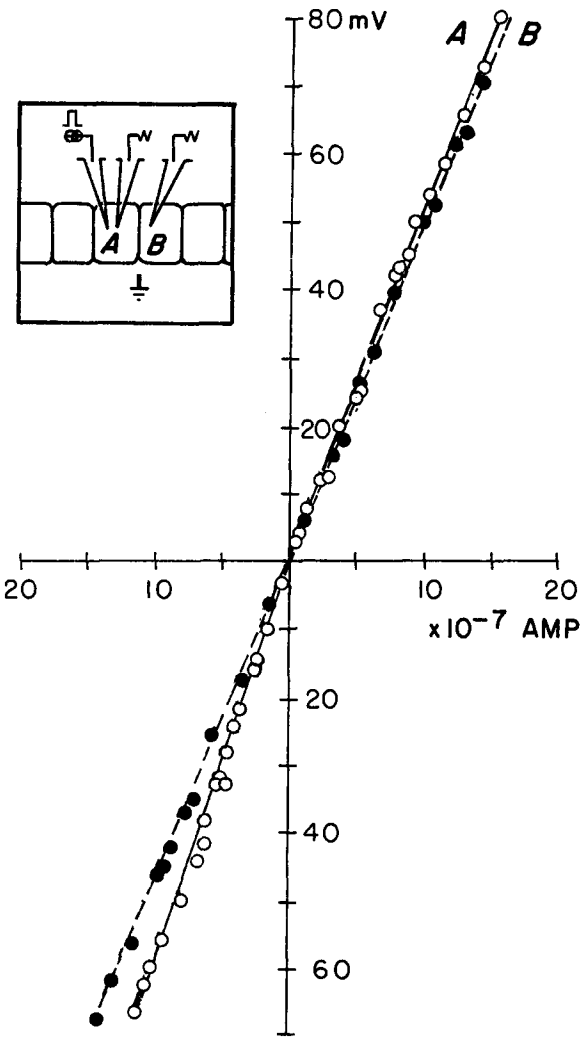

FIGURE 3 Electrical coupling between adjacent cells. Current (abscissae) is passed with a microelectrode between cell A, across the cell membranes of this cell, and the extracellular fluid, and the resulting voltage drops (ordinates, "steady state" voltage) are recorded simultaneously across the surface membranes of cells A and B. (A is at caudal end of the gland.) Outward current, right; depolarization, upwards.

4 KΩ, decreases only slightly from one cell to the next. The slope falls by two orders of magnitude when the cell surface membrane is ruptured experimentally, or when the electrodes are in direct contact with the cell exterior.

For a longitudinal chain of cells, as in this preparation, carrying steady current, the equivalent circuit may, to a first approximation, be given by Fig. 4.[1] The ratio of membrane potential change in the first (A) and second (B) cells, for a given circuit, is then:

$$\frac{V_A}{V_B} = 1 + \frac{2r_c}{r_\parallel} + \frac{r_c}{r_s}\left(1 + \frac{r_c}{r_\parallel}\right), \qquad (1)$$

where r_c represents the resistance between the centers of two adjacent cells across their contact membranes; r_s, the resistance along the intercellular space to the exterior; and $r_\parallel$, the combination of the cell surface membrane resistance (r_o) in cell B in parallel with the entire network to the right.

Three things are then immediately clear from the foregoing experiment: (i) The electrical re-

[1] (to avoid unnecessary complication, the approximation disregards the effect of the lumen and neglects the very small resistance through the external medium).

sistance across the cell surface membrane is high; (ii) The resistance across the cell contact membrane is much lower than that of the surface membrane; (iii) The resistance along the intercellular space to the cell exterior is much greater than that of the contact membranes.

To the reader unfamiliar with electrophysiological problems, these points may perhaps be best made clear by a situation of contrast. Consider, for example, the cases of two adjacent nerve or striated muscle cells in which there is no intercellular coupling. There, the intercellular space is relatively wide, and the resistance along this space low in relation to that of the cell membranes. Current flows then across the resistance of the cell surface membrane (r_o, in the diagram of Fig. 4) directly into the cell exterior (e), and, part of it, across the contact membrane (r_c) into the intercellular space (r_s), from where it is shunted to the cell exterior. Thus, little current enters the adjacent cell *B*. As a result, the membrane voltage recorded from inside *B* is much attenuated. In fact, in many nerve and muscle cells the attenuation is such that membrane voltages become undetectable in an adjacent cell with the ordinary means of amplification.

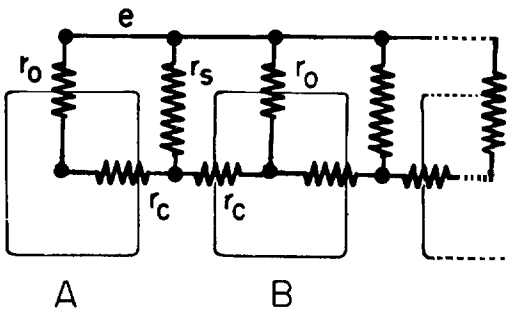

FIGURE 4 Analog of a cell chain. r_o, resistance across the cell surface membrane; r_c, across the cell contact membrane; r_s, along the intercellular space to exterior.

In the present epithelial cells, there is hardly any voltage attenuation. This behavior, so strikingly different from the familiar picture of nerve and muscle cells, was what originally drew our attention to the problem of cell contacts (36). Here, obviously, a large fraction of the current flows from cell *A* into *B*. This implies that there is no appreciable leakage of current along the intercellular space; the resistance across the contact surface (r_c) is low compared to that of the intercellular space to the exterior (r_s).

This is further illustrated by experiments of the kind described in Fig. 5. Current pulses of constant intensity are passed with an electrode in a fixed position in one cell, and the resulting changes in membrane voltage recorded with a roving electrode from inside cells located at varying distances along the approximately cylindrical portions of the gland. To simplify the analysis, current leakage through the luminal cell surface was minimized by insulating the duct electrically from the Shen fluid bathing the gland exterior. For this purpose, the content of the duct was exchanged with an isotonic aqueous solution of sucrose—a medium of very high resistivity—and the end of the duct was kept in a pool of flowing sucrose. (The sucrose pool was separated from the Shen fluid by a barrier of petroleum jelly. The resistance between duct and gland exterior was measured routinely to check insulation.) As is seen in the experiment of Fig. 5, the membrane voltage becomes progressively smaller as one records from more distant cells. But the decrement is only of an order one would expect if the gland with its 200 cells were to behave like a cable conductor with a continuous cytoplasmic core bounded solely by an external insulating membrane. In fact, in those cases in which the gland diameter was small in relation to the space constant of voltage decrement, and in which there were no appreciable voltage drops in the radial dimension of the gland, the agreement with cable theory was fairly good (see next section). In a representative case of a gland of 200 μ diameter (data of Fig. 5), the space constant was 1.2 mm, which is practically the same as that of squid giant nerve fiber at equivalent diameter (*cf.* 7) in which, indeed, there are no core septa or obvious leakage pathways. This, once again, shows that the contact membranes offer low resistance to ion flow, and that the diffusion path to the cell exterior along the intercellular space presents a much higher resistance. It also reveals particularly clearly that the surface membrane of the gland cells has the high resistance of nerve and muscle cell membranes.

SURFACE RESISTANCE: The surface resistance may now be evaluated. The resistance network in Fig. 4 is given to account for the steady-state potential distribution in the gland cells due to a constant current supplied by an intracellular

electrode. Although introduced with reference to a longitudinal chain of cells, the same kind of network should be equally applicable to the entire gland, since this can be represented by several such chains of cells with their corresponding network elements in parallel.

In the present case, the ratio of the gland diameter to the space constant of the longitudinal voltage distribution is only 0.16. One may, therefore, neglect radial variation of potential within the gland. We neglect also the field distortion due to the presence of a dielectric (sucrose solution) in the lumen, since the lumen occupies less than 3 per cent of the cross-sectional area over most of the gland length. The external medium, an electrolyte solution grounded through a large electrode, may be considered isopotential. The boundary conditions are specified by the constant internal current source at the end of the gland and by the insulation from the external medium at the other end.

Since the gland length is only 1.3 times the space constant, the (single) exponential expression for the potential distribution, which has been so frequently useful in dealing with nerve and muscle fibers (*cf.* 18, 12), is not sufficient here. The expression which satisfies the differential equation and the boundary conditions for so short a cable is:

$$V = V_o \frac{\cosh \frac{L - x}{\lambda}}{\cosh \frac{L}{\lambda}}; \quad \text{(see Appendix).}$$

Here, V, the change of potential across the gland surface due to the steady current, is proportional to a hyperbolic cosine function of x, the distance along the gland axis, measured from the position

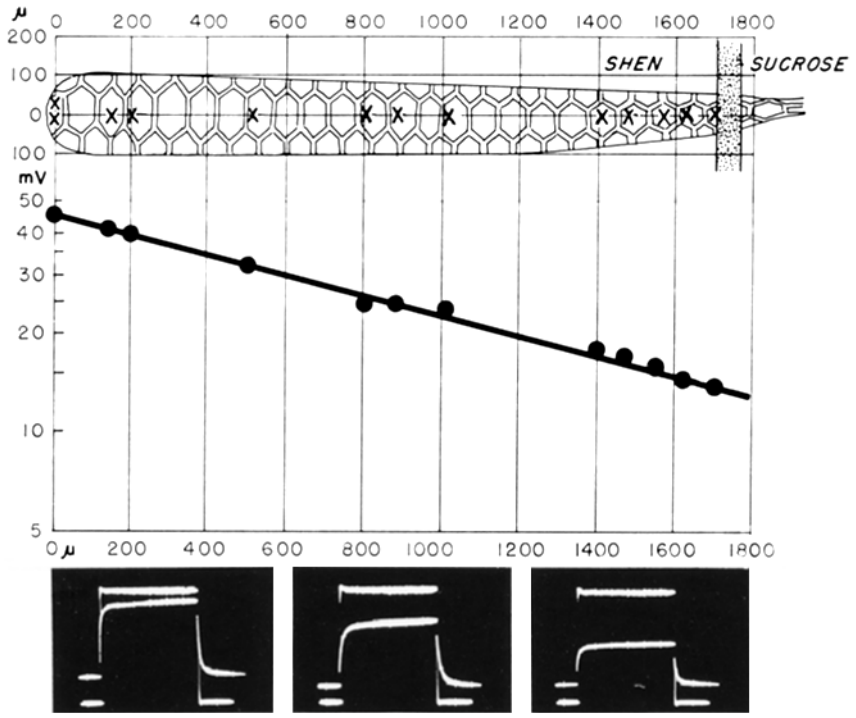

FIGURE 5 Membrane voltage attenuation along a cell series. Current is passed with an electrode in one cell (length 0 on the abscissae) and the resulting changes in "steady-state" voltage (ordinates) are recorded across the membranes of cells located at varying distances (abscissae) from the current source. Gland duct filled with sucrose to avoid current leakage through the luminal cell surface. *Upper inset:* camera lucida drawing of the gland epithelium; the crosses denote points of electrode insertion. *Lower inset:* samples of records of membrane current (upper beam) and membrane voltage (lower beam) at, from left to right, lengths 0, 200, 800 μ. Duration of rectangular pulse of current, 60 msec.

of the current source. V_o is the value of V at $x = 0$. L is the gland length and λ, the space constant. (Here, of course, λ cannot be considered as the length corresponding to attenuation $1/e$, as in the case of the single exponential expression.)

The resistance of unit gland surface R_m is then:

$$R_m = \left(\frac{\lambda V_o}{I_o} \tanh \frac{L}{\lambda}\right) \cdot (\text{circumference}),$$

as shown in the Appendix; I_o is the total input current.

ances ranging between 10,000 and 12,000 Ω cm². The values of surface resistance may be compared with the resistance values (uncorrected for membrane infoldings) available for striated muscle (12, 31 *cf.* 17), nerve (8, 16, 17, 38, 72) and egg cells (28, 37, 66) which range between 1000 and 12000 Ω cm².

To make certain that the sucrose treatment in the preceding experiments did not produce substantial alteration in the permeability of the cell membranes, experiments similar to those above were carried out in absence of sucrose. In these

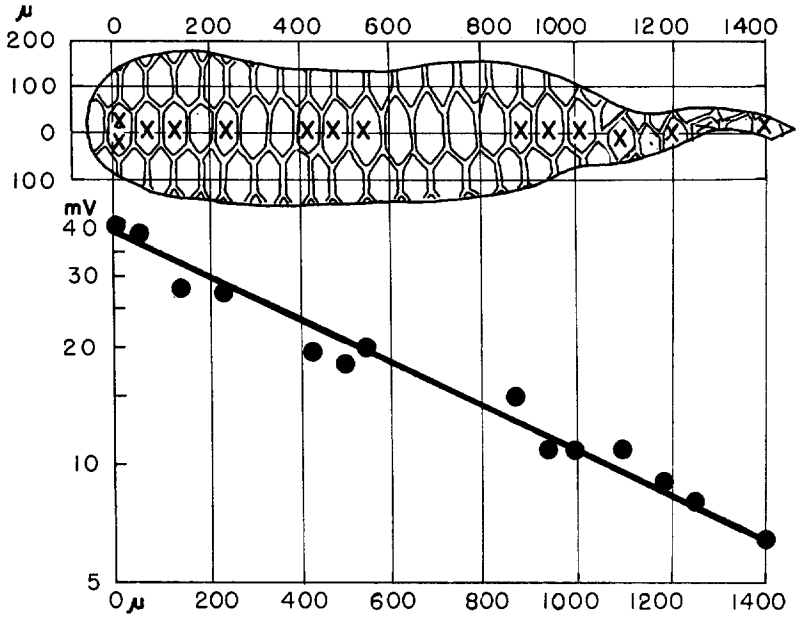

FIGURE 6 Membrane voltage attenuation in a control cell series in absence of sucrose. Procedure and notations as in Fig. 5, except that here both the cell surface membrane and luminal membranes are in contact with Shen's solution.

The experiment of Fig. 5 leads thus to a value of 380 Ω cm² for the surface resistance, and that of Fig. 8 to 390 Ω cm² (see Appendix).

In estimating R_m, the gross linear dimensions of the gland were used. Electron micrographs show, however, that the cell surface membrane is infolded (73) and that the mean length of the unfolded membrane is increased by a factor of approximately 5.5. Thus, the apparent value of the gland surface area is to be multiplied by the square of this factor to give the resistance of unit area. The actual surface resistances are thus 11,400; 11,700 Ω cm². Three other cases, calculated with less precision than those above, gave resist-

experiments, the gland exterior as well as the duct was directly in contact with Shen's solution. The resistance from duct center to exterior was typically around 50 KΩ. With the additional leak of the luminal cell surfaces, the voltage attenuation, of course, is more pronounced; but, as is seen in the example of Fig. 6, the voltage attenuation is still of the same low order as in the preceding experiments.

INTERCELLULAR CONTINUITY: A variation of the above experiments is to flow current directly through the cell interiors of adjacent cells (see arrangement *II* of Methods). In this arrangement, the cell exterior is effectively bypassed as a

current path, and current flows from cytoplasm to cytoplasm across the contact surfaces. The gland lies in oil. Resistance is measured over varying distances along a series of cells at the roughly cylindrical portion of the gland. The results of a typical experiment are given in Fig. 7 (gland diameter 200 μ). The resistance increases roughly linearly with distance over this range shorter than the space constant. The slope is 0.5×10^6 Ω/cm, which corresponds to a resistivity of 160 Ω cm. This is merely of an order of resistivity one would expect from a cylinder of cytoplasm in absence of cell contact membranes. The resistivity of extruded cytoplasm is 100 Ω cm, not much smaller than that of the cytoplasm–contact membrane complex.

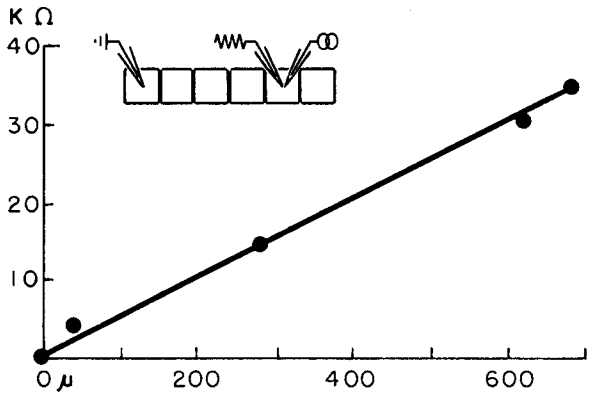

FIGURE 7 The resistance of the cytoplasm–contact membrane complex. Resistance is measured in a cell chain between an electrode ($\frac{\perp}{=}$) fixed inside a cell at the caudal end of the gland and a roving electrode inserted at varying distances (abscissae) along the chain. At point 0, the measuring electrodes were within 2 μ on the surface of the same cell. The following measurements were made over spans of, from left to right, 1, 5, 10, 11 cells. Ordinates give the resistance after subtraction of the resistance of the measuring electrode ($\frac{\perp}{=}$), constant within 2 KΩ. Accuracy of resistance measurements about the size of the dots.

A similar result is obtained if the resistivity (R_i) of the gland core is calculated from the cable model, where:

$$R_i = \frac{V_o}{\lambda I_o} \tanh \frac{L}{\lambda} \text{ (cross-section area)}$$

(see Appendix).

The data from the experiment illustrated in Fig. 5 give a value of resistivity for the cytoplasm–contact membrane complex (in the axial direction) of 110 Ω cm, and that from the experiment in Fig. 8 a value of 190 Ω cm, as against that of 100 Ω cm of extruded cytoplasm. The values of two other glands, calculated with less precision, were 120 and 160 Ω cm.

These results bring out with particular clarity the lack of any substantial barrier between cells.

CELL INJURY AND INTERCELLULAR CONTINUITY: The ionic continuity between epithelial cells manifests itself also in another way. If the surface membrane of one cell is injured by experimental or accidental perforations, the resting potential of this cell falls to zero, and, with delays depending on distance, the other cells of the gland follow suit. This is usually accompanied by a visible clouding of the cells which spreads progressively over the gland.

INTERCELLULAR SPACE RESISTANCE AND CELL SURFACE MEMBRANE RESISTANCE: As already noted, the surface resistance determined in the experiments on voltage attenuation of the type illustrated in Fig. 5 is the parallel combination of the cell surface membrane resistance and the intercellular space resistance. Both are clearly of a high order of magnitude. The lower limit for both is the gland surface resistance 10^4 Ω cm^2. But their relative magnitudes are not revealed by the foregoing experiments. In the following experiments, an attempt is made to resolve these components by the use of a method of greater space and voltage resolution, and one which does not rest on cable properties of the gland alone. The gland duct was filled with sucrose. One micropipette passed current between cytoplasm and the exterior. Another electrode recorded intracellularly the membrane potential change at points along the gland surface as illustrated in Fig. 8. The size of the cell allowed us to determine the differences of membrane voltage across two successive intervals within the cell and an interval straddling an intercellular gap. The points of electrode insertion lay in the plane of the gland axis, and the depths of insertions were up to 5 μ. The data are given in Table I. As is seen in the two examples of Fig. 8, there are no signs of greater

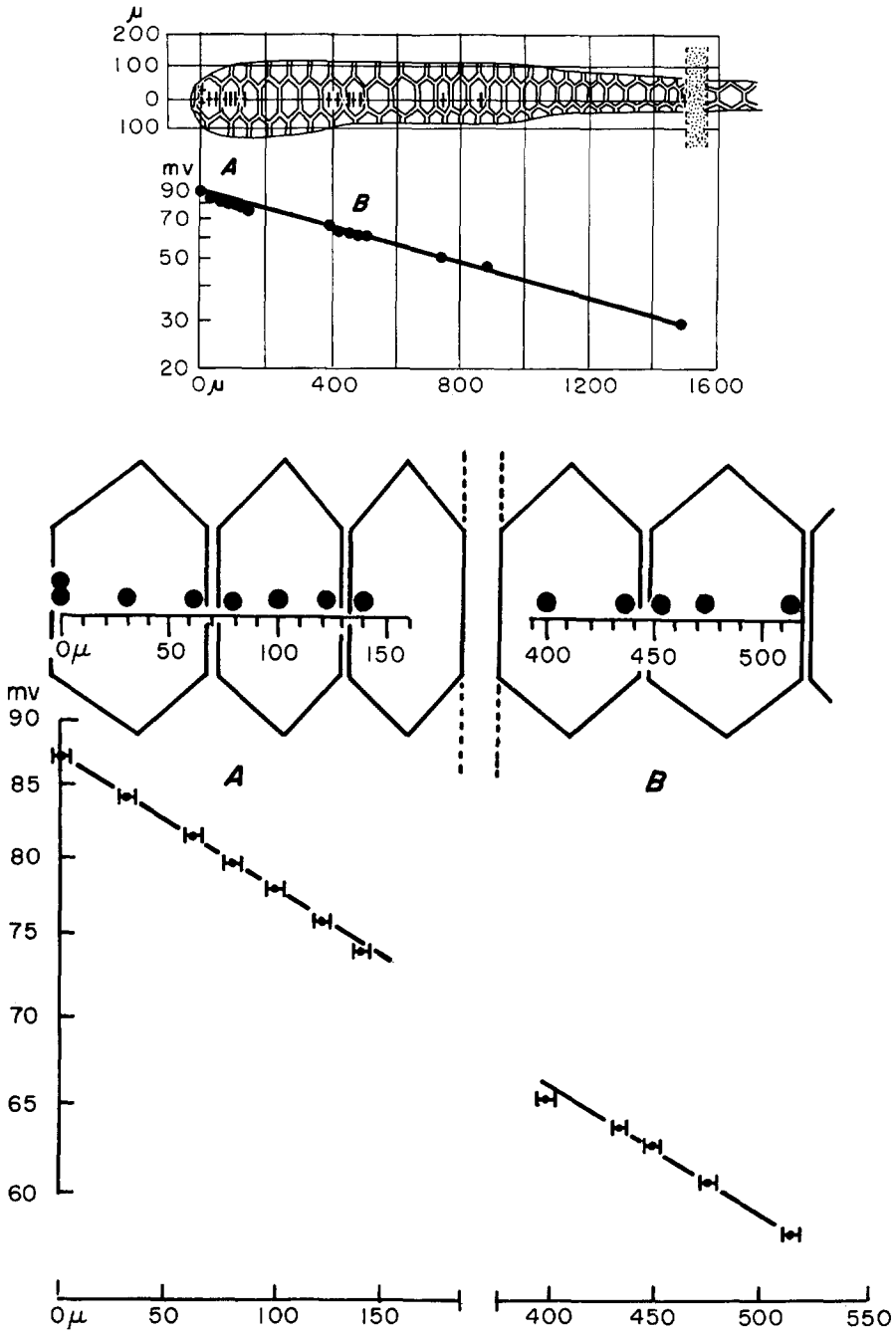

FIGURE 8 Intercellular space and cell surface resistance. A current-passing electrode (fixed position) is inserted into one cell (distance 0) and membrane voltages are recorded intracellularly at points as indicated on the upper inset and on expanded scale between the regions *A* and *B*. Upper and lower insets are camera lucida drawings. Intervals between successive recording points fall either within a given cell or across an intercellular gap. In the latter case, points were chosen to be at least 5 μ from the contact border visible under the light microscope, to allow ample margin of safety for cell overlapping at the contact border (cell extensions do not overlap beyond a fringe zone of 0.8 μ, as seen under the electron microscope (73). *Ordinates:* mean membrane voltage of various successive determinations (see Table I); standard error less than 0.3 per cent. *Abscissae:* distance; bars subtend standard error.

current leakage at an intercellular gap than at the cell surface membrane; all voltage points fall sensibly along a single smooth curve, regardless of whether they are recorded at the edge of an intercellular space.

The accuracy of the voltage measurements is high. The standard error of the voltage difference determinations is, in all cases, less than 0.5 per cent. The serious limitation of the method is its low spatial resolving power because of dimpling of the surface under the electrode tip; the distance measurements have an accuracy of ± 5 μ. The experiments reveal, in any event, no local variations in leakage along the gland surface. The relative magnitudes of the cell surface membrane resistance and intercellular space resistance remain unresolved. The membrane resistance values for a wide variety of other cells, however, all fall within one order of magnitude, 10^3–10^4 Ω cm^2. There is no reason to expect that the resistance of the present cell surface membrane is vastly different, especially since the surface resistance of the gland falls within this range. Since the lower limit for the intercellular space resistance, expressed as surface resistance, is itself about 10^4 Ω cm^2, the actual magnitude is evidently at least as large as that of the cell surface membrane.

TABLE I

Data of Experiment of Fig. 8

Distance	mv	Standard error	No. of determinations
μ			
0	87.07	±0.26	8
32	84.15	±0.38	10
63	81.91	±0.195	5
79	80.00	±0.0	9
100	78.40	±0.25	3
122	76.59	±0.0	4
139	73.95	±0.06	4
400	65.30	±0.30	11
437	64.76	±0.226	11
452	63.76	±0.09	8
475	62.10	±0.156	8
515	59.14	±0.05	7

Tracer Experiments

The question of the diffusion resistance along the intercellular space and through the contact membranes was also approached with tracer particles. The choice of a tracer for the present purpose was guided by its particle size, its mobility, and the ease of its detection. We used fluorescein sodium. Fluorescein sodium has a molecular weight of 376. It diffuses readily through cytoplasm and is traceable, by its fluorescence in ultraviolet light, in concentrations as low as 10^{-8} M.

The glands were isolated and placed in Shen's solution as in the preceding experiments. Approximately 5×10^{-9} cc of 10 mM fluorescein were injected into one cell of the gland. This was initially clearly visible as a fluorescent bleb around the micropipette under the microscope. From this bleb, the fluorescence was invariably found to extend in all directions through the cytoplasm of this cell and through the cytoplasms of adjacent cells of the gland. Within 10 to 20 minutes, all cells, except a few near the duct, became fluorescent (Fig. 9). No fluorescein leaked out to the cell exterior.

To observe possible leakage through the basal or luminar surface of the gland, the gland was moved from time to time to a fresh bath, and the bath scanned for fluorescence. This was a fairly sensitive method: when a cell was punctured experimentally, leaks to the exterior could be detected through single holes of 2 to 5 μ diameter. In intact cells, fluorescein never appeared in the bathing fluid, nor in the duct fluid. This corroborates for fluorescein what the preceding electrical measurements had shown for ions normally present in the epithelium.

The cell volume (single cell) into which the 5×10^{-9} cc of fluorescein (10 mM fluorescein in Shen's solution) was injected was about 350×10^{-9} cc, and the total gland volume about 200 times greater. Thus, the injection of fluorescein must have caused an initial change in osmolarity of the injected cell of less than 0.1 per cent, and, after final dilution into the whole gland, a change of less than 0.0005 per cent. This is the great advantage of fluorescein as a tracer; it is detectable with ease at so low concentrations which have no apparent deleterious effects. In fact, even after repeated injections of fluorescein, we found no signs of cell damage; the cell volume, the cell transparency, and the cell membrane potentials, all appeared unaltered.

The fluorescent yield of fluorescein diminishes with increasing concentration. This is due to resonance effects in between its molecules, and is a general phenomenon in aromatic substances

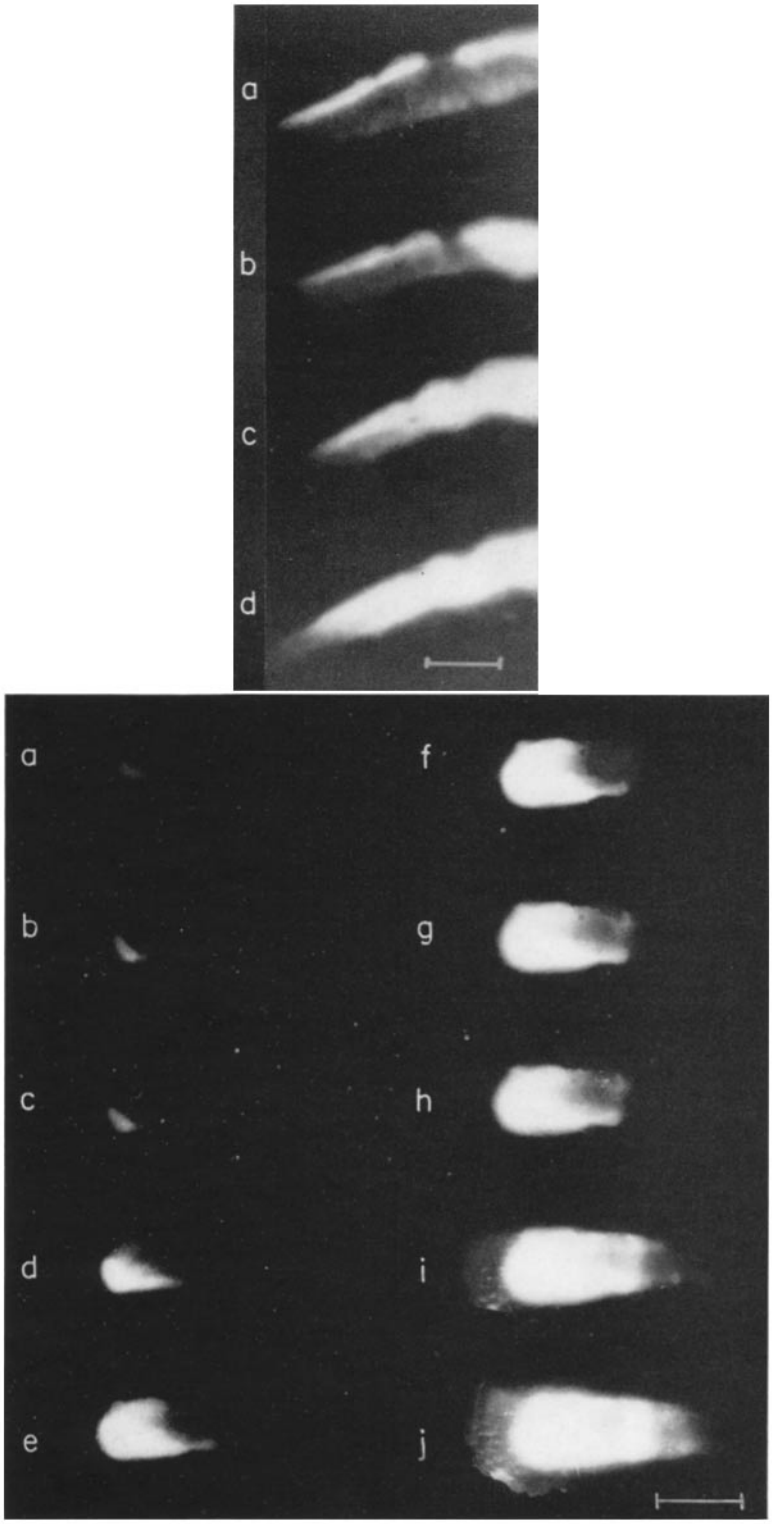

FIGURE 9

(*cf.* 52 *a*). This quenching of fluorescence is visible particularly clearly in the bottom illustration of Fig. 9. Here the the fluorescence of a given volume of fluorescein is seen increasing from *a* to *j*, as the ions dissolve into an increasing cell volume. In the original concentration inside the micropipettes (10 mM), the fluorescence is too feeble to be detected by the photographic film at the exposure times used, and for this reason the outlines of the pipettes are not visible in the figures. To the eye, the fluorescence is, however, clearly visible, which helped us greatly in maneuvering the pipettes inside the cells.

DISCUSSION

DIFFUSION BARRIER BETWEEN INTERCELLULAR SPACE AND EXTERIOR: Our most striking finding is that ions move rather freely from one epithelial cell to another, but not so from the intercellular space to the exterior. The electrical measurements and fluorescein experiments show clearly that the intercellular space, or at least a part of it, is sealed off from the exterior by a strong barrier. The structure that here immediately suggests itself as a possible barrier is the *septate junction* on the luminal end of the intercellular space, described in detail in the subsequent paper (73) of this series. At the level of the *septate junction*, the intercellular space is narrow (150 A) and is interrupted transversely by parallel bridges of structured material, the *septa* (Fig. 10). Indeed, an arrangement in which the contact membranes are joined by a long series of septa (there are about 2,000 septa per cell junction) would make an ideal seal, even if the material of which the septa are made had a specific resistance lower than that generally presented by cell surface membranes.

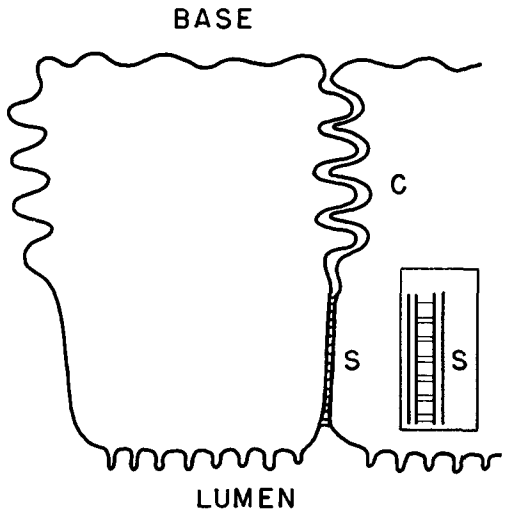

FIGURE 10 Scheme of a cell junction. *C*, convoluted region at which cell surfaces interdigitate. *S*, septate junction at which unit membranes appear joined periodically.

A point of comparison are the *terminal bars* of mucosal, glandular, and duct epithelia of mammals (*cf.* 10). In a remarkable paper, Farquhar and Palade (10) showed that the outer membrane complexes merge at certain regions of the terminal bars, the *zonulae occludentes* of these authors, and,

FIGURE 9 Intercellular diffusion of fluorescein.

Top. Approximately 5×10^{-9} cc of a 10 mM fluorescein solution is injected into a cell slightly off-center to the right, the caudal end of the gland. (This amounts to about 1/60 of the cell volume.) Ultraviolet rays are projected obliquely onto the gland through a darkfield condenser, and the scattered fluorescence is photographed at equal film exposure times: *b*, 2 minutes; *c*, 18 minutes; *d*, 30 minutes after fluorescein injection. *a*, gland before injection. Some of the adventitious tissue in this preparation is normally fluorescent, giving an outline of the gland in ultraviolet. In *d*, the outlines of the duct are visible. Calibration: 300 μ.

Bottom. Another case. Here, with the intensity of ultraviolet used there is little natural fluorescence in the adventitious gland tissues. Photomicrographs *a*, at the moment of injection of about 5×10^{-9} cc of 10 mM fluorescein-Na into one of the 200 cells of the gland. *b*, 2 minutes; *c*, 4 minutes; *d*, 6 minutes; *e*, 8 minutes; *f*, 10 minutes; *g*, 12 minutes, *h*, 14 minutes, *i*, 16 minutes; *j*, 18 minutes after injection. The decrease in fluorescence from *j* to *a* is due to concentration quenching of fluorescence (See text). Calibration: 300 μ.

Note the absence of fluorescence in the fluid bathing the gland in both cases.

in the cases of renal tubular and pancreatic duct epithelia, pin-point the diffusion barrier for hemoglobin and zymogen at these regions.

The *septate junction* may well be the only existing seal between intercellular space and exterior. In fact, if the septate junction is also the site of an increase in intercellular permeability (see below), no other seal is required to explain our results. But since our results give proof only of the existence of a path of low resistance at the contact surface of cells, but not of its precise location, we will consider briefly the possibility of a second membrane seal toward the basal side. An arrangement of this kind is pertinent, if the primary path of low resistance is located at a central region of the contact surfaces, for instance, at the convoluted portion.

Towards the convoluted portion of the intercellular space (*convoluted region*), there is no such clear structural candidate for a seal. There, the intercellular gap is often as wide as 450 A, although, at points, the contact membranes are seen to come close together (73). Whether the membranes merge at such points cannot be ascertained; the contact surfaces are too intertwined, and the surface relations too complex. In any event, there is no continuous structural arrangement demonstrable under the electron microscope, that suggests the presence of a barrier along the basal edge. Another possibility as a barrier is a narrow diffusion path along the intercellular space. But in order to make an effective barrier, such a path, if filled with ordinary extracellular fluids, in addition to being narrow, must, of course, also be much longer in the lumen-to-base direction of current flow (*length*) than in the dimension parallel to the cell surface membrane (*depth*). This excludes immediately a continuous intercellular space as a barrier. Given the perimeter of the basal cell face, the base-to-lumen height of the cells, and the length and orientation of the interdigitating cytoplasmic processes, as seen in electron micrographs (73), a continuous intercellular space in the present case will, in all likelihood, have a *length-depth* ratio less than 1, and, certainly, not greater than 1. Consequently, if a diffusion barrier exists at all at the convoluted region, one is left with only one possible arrangement, that of a tortuous but continuous commissure of contact membranes forming a long and narrow path in which the depth resistance component amounts to only a negligible fraction of the length component.

Another structure to be considered as a possible barrier is the basement membrane. This is the web that envelopes the entire gland and represents the only structural separation between cell membrane and exterior (73)[2] We have systematically explored the surface resistance of the gland in an attempt to see whether there is a resistance component in addition to that of the cell membrane. In these experiments, we used electrodes of specially fine tips, of the type employed in our nuclear membrane work (36). One electrode, inserted inside a gland cell, pulsed current continuously across the gland surface, while a second electrode, advancing progressively through the gland surface, recorded the corresponding voltage drops. The recording electrode was driven at a deliberately slow speed with the hydraulic advance mechanism of our micromanipulator. In all cases, only one resistance step was discernible (Fig. 11). A negative result is, of course, not conclusive. But we should like to point out that the technique has a resolving power much greater than that which one may expect *a priori*. With this technique we were able to discriminate, for example, a series of two resistances in a pair of overlapping surface membranes, separated by a space not unlike the present one (28).

The possibility of the basement membranes being a diffusion barrier is also unlikely for other reasons. Loose collagen tissue, in general, and basement membranes, in particular, are known to be permeable structures. In basement membranes of capillary endothelia there is evidence for high permeability to ions (*cf.* 40, *cf.* 49) and even to large molecules (11); and in basement membranes of skin, to ions (67).

INTERCELLULAR PERMEABILITY: The low diffusion resistance for ions found across the cellular contact surfaces may mean two things: (i) The specific membrane resistance, *i.e.*, the resistance of unit area of membrane is lower at the cell contact membrane, or at regions thereof, than at the cell surface membrane. This, an actual increase in permeability, is a good possibility, since the resistance of the contact membrane is so extraordinarily low. In fact, the resistance across a series of contiguous cells did not measure substantially more than in cytoplasm without contact

[2] Over a narrow zone of the gland, there are also some fat and additional connective tissue. But this zone encompasses only few cells, which were avoided in our experiments. The zone is easily distinguished under the light microscope by its lack of transparency.

membranes. (ii) The specific membrane resistance is similar at all cell surfaces, but the total area of membrane over which the resistance is measured is very much larger at the contact surface than at the outer surface. Electron micrographs show that the cell surface membrane and, particularly, the contact membranes are infolded. The total area of contact membrane may well be larger than that of the cell surface membrane. But the question is whether the difference is large enough to account for the observed value of resistance. An accurate estimation of the area of contact membrane cannot be made; the surface relations are too intricate. But one can estimate an upper limit of the contact area. This allows one to decide between the two possibilities. A membrane wrapped straight around the contact surface of the cell would have an area of the order of 10^{-4} cm^2; and, with a specific resistance of the order of 10^4 Ω cm^2 as that of the surface of the epithelium, would offer a resistance of the order of 10^8 Ω. The actual resistance measured across the contact membrane is 10^3 Ω. Hence, to account for this resistance on the basis of a surface expansion, the condition is that the contact surface be enlarged by at least 5 orders of magnitude. The electron microscope reveals the convoluted junction to consist of cell extensions, finger-like, and laminar projections up to 0.4 μ long (most are shorter) (73). The distance between the membranes of a given extension ranges from 1,400 to 8,500 A, and the intercellular space between extensions, from less than 100 to 450 A. All surface packing occurs within a limiting zone of 1 μ; this is the zone along the cell perimeter beyond which clearly no extensions occur. Thus, in the most efficient surface packing—one extension lying next to the other—the upper limit of contained surface lies between 10^{-4} and 10^{-3} cm^2. This falls short of the required surface by 4 to 5 orders of magnitude. To illustrate this further, consider the cases of laminar or finger-like packing in which there is a membrane every 100 A, a packing so dense that there is virtually neither cytoplasm inside nor gap between extensions. Even in such an absurdly close packing, the area falls short by 2 orders of magnitude. *It is clear, therefore,*

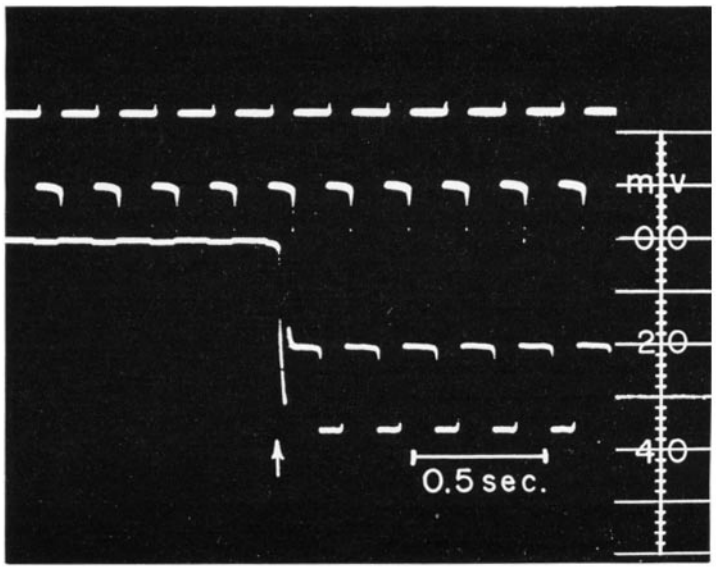

FIGURE 11 Surface barrier. Current pulses (upper beam) of constant strength (7×10^{-8} amp) are passed continuously between an intracellular microelectrode and the cell exterior. The membrane potential (lower beam) is recorded between a reference electrode in the extracellular fluid and a second microelectrode advancing progressively in the direction cell exterior–interior. The crossing of the cell boundary by the electrode (arrow) coincides with the abrupt appearance of the resting potential and of large voltage pulses across a surface resistance which is 228 KΩ in this case. Note that there is only a single resistance step at the gland cell surface.

that the specific cell membrane resistance is lowered at the contact surfaces. The large contact area may contribute to some extent to the low (effective) resistance, but the essential and novel point is that the actual permeability of the cell membrane is markedly changed at the zones of contact. The difference in permeability is, at least, of four orders of magnitude; while the upper limit of conductance for the cell surface membrane is of the order of 10^{-4} mho/cm^2, the lower limit for the contact membranes is of the order of 10 mho/cm^2.

The same conclusion follows from a similar line of reasoning applied to the results on attenuation of membrane voltage (Fig. 5). This, of course, constitutes no basic independent evidence if the model of Fig. 4 is taken to apply. But it is nonetheless satisfying that two different kinds of measurement yield the same result.

A change in membrane permeability implies a special modification in the build-up of the surface membrane. A possible site is the *septate junction* at which the surface structure, as given by electron micrographs, is evidently modified and where the intercellular gap is smallest (73). One may speculate, for instance, that the "septa" circumscribe diffusion channels in the cell-to-cell direction across the intercellular space. An important point in this connection, which is still unclear, is whether the "septa" are continuous belts along the cell perimeter. If they are continuous, one may possibly think of the septate junction as an alternating sequence of materials of low and high resistivity. Indeed, an arrangement of this sort would make a good ionic coupling device. In the cell-to-cell direction of ion flow, there are many in-parallel channels which will lower the diffusion resistance, while in the direction of intercellular space to exterior, there is a long series of barriers. This arrangement would provide a diffusion path as well as a seal. A coupling of this kind implies either that the resistivity of the material in the intercellular space between septa be low, while that of the electron dense septa be relatively high (although not necessarily as high as that of unit membranes); or the reverse. If, on the other hand, the "septa" are pin-like structures, an attractive picture that suggests itself is that of pins with a core of low resistivity coated with a material of high resistivity. In an arrangement of this kind, each "septa pin" may be an aqueous channel sheathed in a circumferential diffusion barrier, after the pattern of, for example, simple liquid-crystalline phases of certain phospholipids, in which molecules appear oriented at certain temperatures in hexagonal arrays of cylinders with central water channels (38 *a*, 61 *a*). A coupling device of this sort again provides many in-parallel diffusion channels and a diffusion barrier to the intercellular space. But it differs in a major aspect from the coupling type with continuous "septa." The barrier is not necessarily continuous in the base-to-lumen direction of the intercellular space. It is only a continuous barrier for diffusion between the intercellular channels and the intercellular space (and exterior); and this is the only absolute condition for a barrier set by the results of the present work. It seems fruitless to pursue these speculations into the molecular aspects of membrane permeability at cell junctions until more evidence is available on this point and on the wider problem of the molecular build-up of membranes in general. But it is noteworthy that front views of the septate junction show regular patterns suggesting a polygonal or circular unit array (see Fig. 9 of the subsequent paper of this series) whose dimensions fall within the range of the arrays of the aforementioned lipid-water phases; and which may be compared with the arrays described by Sjöstrand in mitochondrial and certain intracellullar membranes (60 *a*) and by Robertson in synaptic junctions of the Mauthner cell (55 *b*). It should be rewarding, perhaps, even in sight of the wider problem, to expend further effort in studies of birefringence and of electron and x-ray diffraction of close membrane junctions.

Other regions of the contact surface at which there is visible modification of the surface membrane under the electron microscope, and which, therefore, may suggest themselves as sites of modified membrane permeability, are the desmosome-like structures in the convoluted contact surface. Although there is nothing in our results to exclude this, it seems to us not a likely possibility, in view of the results of Kuffler and Potter (34) in neuroglia-nerve cell associations in the leech. There are numerous desmosomes binding glia to nerve cells, but Kuffler and Potter find no electrical coupling between these two kinds of cells. (In glia-to-glia junctions, however, these authors find a close coupling.)

GENERAL CONDITIONS FOR INTERCELLULAR COUPLING: The determining factors of electrical (ionic) intercellular coupling are depicted quite in general in the circuit diagram of

Fig. 4, and their relations are given by equation *1*. One of the factors, the cellular surface resistance (r_o), is high and rather similar in most cell systems. The degree of cell-to-cell coupling depends thus chiefly on the resistance of the contact membrane (r_c) and the resistance along the intercellular space (r_s). Good coupling requires a low r_c and a relatively high r_s. A high r_s may result from close membrane apposition (maximal r_s in this case obtains when the intercellular space is absent), or from occlusion of part of the intercellular space by material of high electrical resistivity (not necessarily recognizable under the electron microscope). The size of the intercellular gap is, therefore, alone not a deciding factor in determining the degree of electrical coupling. This should be realized when one tries to identify an electrically coupled junction on the basis of morphological criteria. Proximity between contact membranes is, of course, in all likelihood, a general morphological feature of electrically coupled junctions, but not necessarily an exclusive one. The second condition, a low r_c value, may result from a low specific resistance of the contact membranes, an enlargement of contact membrane area, or a combination of both. Strong coupling is likely to be always associated with a low specific resistance, since, as in the present junction and discussed above, the area of contact membrane is generally not large enough for the required lowering of r_c. Recognition of variations in specific membrane resistance is, at this time, beyond the reach of the electron microscope. Thus, the only safe criterion for identification of an electrically coupled junction, and one that at this stage defines best such a junction, is provided by determination of resistance to ion flow.

This resistance is particularly small in the present epithelial junction in which ions move nearly as freely as in protoplasma. Here both, a low specific resistance and a large area of contact membrane concur in making a strong coupling. In the two other epithelia heretofore examined, the salivary gland epithelium of Chironomids and the urinary bladder of toad, electrical coupling is present, but is not so strong. In the former, the coupling ratio V_B/V_A of adjacent cells (see equation *1* and Fig. 4) averages 0.79 (early developmental stages) (Higashino and Loewenstein, unpublished) and in the latter, about 0.7 (Kanno and Loewenstein, unpublished), as against 0.96 in the present epithelium. These weaker couplings are in both cases paralleled by smaller areas of contact. A cell junction which elucidates the influence of r_c and r_s particularly well, is the junction that forms during division of an egg cell (*Asterias*). In this case r_c increases progressively and r_s decreases in the process of junction formation, and concomitantly the coupling goes through all stages, from free cell-to-cell diffusion to virtual loss of coupling (1).

SOME GENERAL IMPLICATIONS: In the present epithelial cell associations, cells communicate rather freely with each other, at least so far as some of their ions are concerned. The organ here, rather than the single cell, is the unit of ion environment. This qualification of classical cell theory came as an unexpected side-product of our work. Probably the functional adaptation here is one that allows the cell system to work in concert. Functional control in such a system may possibly be exerted through direct cell-to-cell diffusion of genetic and other factors, with economy of external nervous or humoral controls. The free communication between cells may also be at the root of a number of propagated phenomena known to occur in epithelia upon injury, inflammation, infection etc. (*cf.* 26).

How general the ionic cell communication is remains to be seen in future experiments. Morphologically tight junctions are certainly abundant. Apart from salivary gland cells, they are found in cells of mucosae, pancreas, kidney, mesothelia, to name only a few (*cf.* 10). They are also found in cells of smooth and cardiac muscle (2 *a*, 5 *a*, 7 *a*, 59, 60, 72 *a*, 75 *a*). It may not be too risky, therefore, to foresee ion communication as a widespread property of cell association. The degree of electrical coupling may vary, of course, from system to system, depending on the factors analyzed above. The nerve and striated muscle cells, with their wide intercellular spaces and lack of electrical coupling, are probably the exceptions rather than the rule.

APPENDIX

The potential along the gland can be treated by the standard methods of transmission line analysis. Thus, for the present case, the standard expression will be derived for the distribution of potential across a thin insulating sheath bounding a core conductor of *finite* length. The potential arises from a steady current flowing between an internal electrode at one end of the core and the external

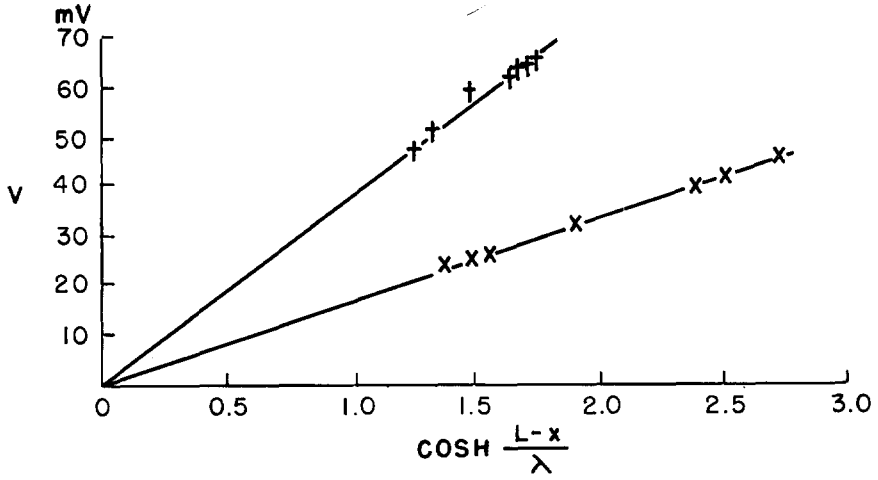

FIGURE 12 Voltage attenuation along length of gland. The lines give the least-square representation, by equation 5 (Appendix), of the experimental data of Figs. 5 (×) and 8 (†), respectively.

medium, assumed a perfect conductor at ground potential. The core is taken to have a uniform cross-section whose diameter is much smaller than the space constant of the longitudinal potential distribution. The distal end of the core conductor is assumed to be insulated from the surrounding medium.

V Potential difference across the insulating sheath at an arbitrary point along the length

x Position along the length of the core conductor measured in cm from the current electrode

V_o The value of V at the current source ($x = 0$)

I Current traversing the core conductor at an arbitrary point

I_o Total current flowing into the core from the internal electrode

L Length of the core conductor

r_m Resistance of unit length of the insulating sheath, in Ω cm

r_i Resistance per unit length of the core conductor, in $\Omega\ cm^{-1}$

R_m Specific resistance of the sheath, in $\Omega\ cm^2$

R_i Specific resistance of the conducting core, in Ω cm

Upon establishment of a steady current from the internal electrode, the potential gradient along the core is:

$$\frac{dV}{dx} = -Ir_i \qquad (1\ a)$$

The loss of current by leakage through the sheath is described by:

$$\frac{dI}{dx} = -\frac{V}{r_m} \qquad (2)$$

Upon differentiating equation (1 *a*) with respect to x and then substituting from equation (2), we obtain:

$$\frac{d^2V}{dx^2} = \frac{r_i}{r_m} V$$

or

$$\frac{d^2V}{dx^2} = \frac{1}{\lambda^2} V \qquad (3)$$

where $\lambda = \sqrt{\frac{r_m}{r_i}}$ is the so called "space constant."

A suitable solution for equation (3) must satisfy also the boundary conditions:

$$\left.\begin{aligned} I &= I_o \quad \text{at} \quad x = 0 \\ I &= 0 \quad \text{at} \quad x = L \end{aligned}\right\} \qquad (4)$$

By substitution in equations (3) and (1 *a*), it is readily seen that:

$$V = V_o \frac{\cosh \frac{L - x}{\lambda}}{\cosh \frac{L}{\lambda}} \qquad (5)$$

is the desired solution provided that:

$$V_o = \frac{I_o\sqrt{r_m r_i}}{\tanh\frac{L}{\lambda}} \tag{6}$$

The hyperbolic functions employed here are defined by:

$$\cosh a = \frac{e^a + e^{-a}}{2} \quad \text{and} \quad \tanh a = \frac{\sinh a}{\cosh a} = \frac{e^a - e^{-a}}{e^a + e^{-a}}$$

Equation (5) has been fitted to the data of Fig. 5 by least squares, and values have been found thus for V_o, L, and λ. This procedure was followed because the diameter of the gland diminishes with increasing x, so that the data cannot be truly represented by a single value of λ and the observed value of L. (Similar results were obtained more recently with the use of Bessel functions).

From equation (6) and the definition of λ:

$$r_m = \frac{\lambda V_o}{I_o}\tanh\frac{L}{\lambda}$$

and

$$r_i = \frac{V_o}{\lambda I_o}\tanh\frac{L}{\lambda}$$

Then

$$R_m = r_m \cdot (\text{circumference of core conductor})$$

and

$$R_i = r_i \cdot (\text{cross-section area of core conductor})$$

All four of these quantities can be evaluated from the least-squared values of V_o, λ, and L, and the observed I_o.

In the case of the data of Fig. 8, the parameters were evaluated for just the seven points between 390 and 900 μ. Since these points lie in a region of almost constant diameter, the calculated parameters should be more precise.

The fit of equation (5) as a description of the data of the experiment of Figs. 5 and 8 may be seen in Fig. 12.

Dr. Kanno is a Visiting Fellow from the Physiology Department of Tokyo Medical and Dental University, Japan.

We thank Dr. S. J. Socolar for many helpful suggestions and discussion on the theoretical treatment of the data.

The work was supported by research grants from the National Science Foundation and the National Institutes of Health.

Received for publication, November 13, 1963.

REFERENCES

1. ASHMAN, R. F., KANNO, Y., and LOEWENSTEIN, W., Intercellular electrical coupling in a forming cell membrane junction of a dividing cell, *Science*, 1964, **145**, 602.

1 *a*. BENNETT, M. V. L., ALJURE, E., NAKAJIMA, Y., and PAPPAS, G. D., Electrotonic junctions between teleost spinal neurons: Electrophysiology and ultrastructure, *Science*, 1963, **141**, 262.

2. BENNETT, H. S., LUFT, J. H., and HAMPTON, J. C., Morphological classifications of vertebrate blood capillaries, *Am. J. Physiol.*, 1959, **196**, 381.

2 *a*. BURNSTOCK, G., HOLMAN, M. E., and PROSSER, C. L., Electrophysiology of smooth muscle, *Physiol. Rev.*, 1963, **43**, 482.

3. BIZZOZERO, G., Sulla struttura degli epiteli pavimentosi stratificati, *Rendi. Real Inst. Lombardo*, 1870, part II, **3**, 16.

4. BUCK, R. C., The fine structure of endothelium of large arteries, *J. Biophysic. and Biochem. Cytol.*, 1958, **4**, 187.

5. BULLOCK, T. H., Properties of some natural and quasi-artificial synapses in polychaetes, *J. Comp. Neurol.*, 1953, **98**, 37.

5 *a*. CASTILLO, J. DEL, DEBELL, J. T., and SÁNCHEZ, V., Electrical behaviour of ascaris muscle cells, *Fed. Proc.*, 1963, **19**, 159.

6. CHAMBERS, R., and RÉNYI, G. S., The structure of the cells in tissues as revealed by microdissection. I. The physical relationships of the cells in epithelia, *Am. J. Anat.*, 1925, **35**, 385.

7. COLE, K. S., Permeability and impermeability of cell membranes for ions, *Cold Springs Harbor Symp. Quant. Biol.*, 1940, **8**, 110.

7 *a*. DEWEY, M. M., and BARR, L., Intercellular connections between smooth muscle cells: the nexus, *Science*, 1962, **137**, 670.

8. ECCLES, J. G., Neurophysiological Basis of Mind, Oxford, Oxford University Press, 1953.

9. FARQUHAR, M. G., and PALADE, G. E., Glomerular permeability. II. Ferritin transfer across the glomerular capillary wall in nephrotic rats, *J. Exp. Med.*, 1961, **114**, 699.

10. FARQUHAR, M. G., and PALADE, G. E., Junctional

complexes in various epithelia, *J. Cell Biol.*, 1963, **17**, 375.

11. FARQUHAR, M. G., WISSIG, S. L., and PALADE, G. E., Glomerular permeability. I. Ferritin transfer across the normal glomerular capillary wall, *J. Exp. Med.*, 1961, **113**, 47.
12. FATT, P., and KATZ, B., An analysis of the end-plate potential recorded with an intracellular electrode, *J. Physiol.*, 1951, **115**, 320.
13. FAWCETT, D. W., Structural specialization of the cell surface, *in* Frontiers in Cytology, (S. L. Palay, editor), New Haven, Yale University Press, 1958, 19.
14. FAWCETT, D. W., and SELBY, C. C., Observations on the fine structure of the turtle atrium, *J. Biophysic. and Biochem. Cytol.*, 1958, **4**, 63.
15. FURSHPAN, E. J., and POTTER, D. D., Transmission at the giant motor synapses of the crayfish, *J. Physiol.*, 1959, **145**, 289.

15 *a*. FURSHPAN, E. J., Electrical transmission at an excitatory synapse in a vertebrate brain, *Science*, 1964, **144**, 878.

16. GRUNDFEST, H., Mechanisms and properties of bioelectrical potentials, *in* Modern Trends in Physiology and Biochemistry, New York, Academic Press, Inc., 1952.
17. HODGKIN, A. L., The ionic basis of electrical activity in nerve and muscle, *Biol. Rev.*, 1951, **26**, 339.
18. HODGKIN, A. L., and RUSHTON, W. A. H., The electrical constants of a crustacean nerve fibre, *Proc. Roy. Soc. London, Series B*, 1946, **133**, 444.
19. GRAY, E. G., Ultra-structure of synapses of the cerebral cortex and of certain specializations of neuglial membranes, *in* Electron Microscopy in Anatomy, (J. D. Boyd, F. R. Johnson, and J. D. Lever, editors), London, Edward Arnold, Ltd., 1961, 54.
20. GRIMLEY, P. M., and EDWARDS, G. A., The ultrastructure of cardiac desmosomes in the toad and their relationship to the intercalated disc, *J. Biophysic. and Biochem. Cytol.*, 1960, **8**, 305.
21. HAGIWARA, S., and MORITA, H., Electrotonic transmission between two nerve cells in leech ganglion, *J. Neurophysiol.*, 1962, **25**, 721.
22. HAGIWARA, S., WATANABE, A., and SAITO, N., Potential changes in syncytial neurons of lobster cardiac ganglion, *J. Neurophysiol.*, 1959, **22**, 554.
23. HAMA, K., The fine structure of the desmosomes in frog mesothelium, *J. Biophysic. and Biochem. Cytol.*, 1960, **7**, 575.
24. HAMA, K., The fine structure of some blood vessels of the earthworm, *Eisenia foedida*, *J. Biophysic. and Biochem. Cytol.*, 1960, **7**, 717.
25. HAMA, K., Some observations on the fine structure of the giant fibers of the crayfishes (*Cambarus virilus* and *Cambarus clarkii*) with special reference to the submicroscopic organization of the synapses, *Anat. Rec.*, 1961, **141**, 275.
26. HARDING, C. V., and SRINIVASAN, B. D., A propagated stimulation of DNA synthesis and cell division, *Exp. Cell Research*, 1961, **25**, 326.
27. HORSTMAN, E., and KNOOP, A., Electronenmikroskopische Studie an der Epidermis. I. Rattenpfote, *Z. Zellforsch. u. Mikr. Anat.*, 1958, **47**, 348.
28. KANNO, Y., and LOEWENSTEIN, W. R., A study of the nucleus and cell membranes of oocytes with an intracellular electrode, *Exp. Cell Research*, 1963, **31**, 149.
29. KANNO, Y., and LOEWENSTEIN, W. R., Low resistance coupling between gland cells. Some observations on intercellular contact membranes and intercellular space, *Nature*, 1964, **201**, 194.

29 *a*. KANNO, Y., and LOEWENSTEIN, W. R., *Intercell. Diffusion Science*, 1964, **143**, 959.

30. KARRER, H. E., Cell interconnections in normal human cervical epithelium, *J. Biophysic. and Biochem. Cytol.*, 1960, **7**, 181.
31. KATZ, B., The electrical properties of the muscle fibre membrane, *Proc. Roy. Soc. London, Series B*, 1948, **135**, 506.
32. KAYE, G. I., and PAPPAS, G. D., Studies on the cornea. I. The fine structure of the rabbit cornea and the uptake and transport of colloidal particles by the cornea *in vivo*, *J. Cell Biol.*, 1962, **12**, 457.
33. KAYE, G. I., PAPPAS, G. D., DONN, A., and MALLET, N., Studies on the cornea, II. The uptake and transport of colloidal particles by the living rabbit cornea *in vitro*, *J. Cell Biol.*, 1962, **12**, 481.
34. KUFFLER, S. W., and POTTER, D. D., Glia in the leech central nervous system. Physiological properties and neuron-glia relationships, *J. Neurophysiol.*, 1964, in press.
35. LING, G., and GERARD, R. W., The normal membrane potential of frog sartorius fibers, *J. Cell. and Comp. Physiol.*, 1949, **34**, 383.
36. LOEWENSTEIN, W. R., and KANNO, Y., Some electrical properties of a nuclear membrane examined with a microelectrode, *J. Gen. Physiol.*, 1963, **46**, 1123.
37. LUNDBERG, A., Microelectrode experiments on unfertilized sea urchin eggs, *Exp. Cell Research*, 1955, **9**, 393.
38. LORENTE DE NÓ, R., A study of Nerve Physiology, Studies from The Rockefeller Institute for Medical Research, **131**, **132**, New York, 1947.

38 *a*. LUZATTI, V., and HUSSON, F., The structure of the liquid-crystalline phases of lipid-water systems, *J. Cell Biol.*, 1962, **12**, 207.

39. MATURANA, H. R., The fine anatomy of the optic

nerve of anurans—An electron microscope study, *J. Biophysic. and Biochem. Cytol.*, 1960, **7**, 107.

40. MAYERSON, H. S., PATTERSON, R. M., MCKEE, A., LEBRIE, J. S., and MAYERSON, P., Permeability of lymphatic vessels, *Am. J. Physiol.*, 1962, **203**, 98.
41. MILLER, F., Hemoglobin absorption by the cells of the proximal convoluted tubule in mouse kidney, *J. Biophysic. and Biochem. Cytol.*, 1960, **8**, 689.
42. MOE, H., The ultrastructure of Brunner's glands of the cat, *J. Ultrastruct. Research*, 1960, **4**, 58.
43. MOORE, D. H., and RUSKA, H., Electron microscope study of mammalian cardiac muscle cells, *J. Biophysic. and Biochem. Cytol.*, 1957, **3**, 261.
44. MUIR, A. R., An electron microscope study of the embryology of the intercalated disc in the heart of the rabbit, *J. Biophysic. and Biochem. Cytol.*, 1957, **3**, 193.
45. MUIR, A. R., and PETERS, A., Quintuple-layered membrane junctions at terminal bars between endothelial cells, *J. Cell Biol.*, 1962, **12**, 443.
46. MUNGER, B. L., The ultrastructure and histophysiology of human eccrine sweat glands, *J. Biophysic. and Biochem. Cytol.*, 1961, **11**, 385.
47. ODLAND, G. F., The fine structure of the interrelationship of cells in the human epidermis, *J. Biophysic. and Biochem. Cytol.*, 1958, **4**, 529.
48. OVERTON, J., Intercellular connections in the outgrowing stolon of cordylophora, *J. Cell Biol.*, 1963, **17**, 661.
49. PAPPENHEIMER, J. R., Passage of molecules through capillary walls, *Physiol. Rev.*, 1953, **33**, 387.
50. PEACHEY, L. D., and RASMUSSEN, H., Structure of the toad's urinary bladder as related to its physiology, *J. Biophysic. and Biochem. Cytol.*, 1961, **10**, 529.
51. PETERS, A., Plasma membrane contacts in the central nervous system, *J. Anat.*, 1962, **96**, 237.
52. PORTER, K. R., Observations on the fine structure of animal epidermis, *in* Proceedings of Third International Conference on Electron Microscopy, (R. Ross, editor), London, Royal Microscopical Society, 1956, 539.

52 *a*. PRINGSHEIM, P., Fluorescenz und Phosphorescenz im Lichte der neueren Atom Theorie, Berlin, Springer Verlag, 1928.

53. ROBERTSON, J. D., The molecular structure and contact relationship of cell membranes, *Progr. Biophysics* and *Biophysic. Chem.*, 1960, **10**, 343.
54. ROBERTSON, J. D., The unit membrane, *in* Electron Microscopy in Anatomy, (J. D. Boyd, F. R. Johnson, and J. D. Lever, editors), London, Edward Arnold, Ltd., 1961, 74.
55. ROBERTSON, J. D., Ultrastructure of excitable membranes and the crayfish median-giant synapse, *Ann. New York Acad. Sc.*, 1961, **94**, 339.

55 *a*. ROBERTSON, J. D., and BODENHEIMER, T. S., The ultrastructure of Mauthner cell synapses and nodes in brains, *J. Cell Biol.*, 1963, **19**, 159.

55 *b*. ROBERTSON, J. D., The occurrence of a subunit pattern in the unit membranes of club endings in Mauthner cell synapses in goldfish brains, *J. Cell Biol.*, 1963, **19**, 201.

56. SCHÄFFER, J., Das Epithelgewebe, *in* Handbuch der mikroskopischen Anatomie des Menschen, Berlin, Springer, 1927, II/1, 1.
57. SELBY, C. C., An electron microscope study of the epidermis of mammalian skin in thin sections. I. Dermo-epidermal junction and basal cell layer, *J. Biophysic. and Biochem. Cytol.*, 1955, **1**, 429.
58. SHEN, T. H., Zytologische Untersuchungen über Sterilität bei Männchen von Drosophila Melanogaster und bei F_1-Männchen der Kreuzung zwischen D. Simulans-Weibchen und D. Melanogaster-Männchen, *Z. Zellforsch. u. Mikr. Anat.*, 1932, **15**, 547.
59. SJÖSTRAND, F. S., and ANDERSSON, E., Electron microscopy of the intercalated discs of cardiac muscle tissue, *Experientia*, 1954, **10**, 369.
60. SJÖSTRAND, F. S., ANDERSSON-CEDERGREN, E., and DEWEY, M. M., The ultrastructure of the intercalated discs of frog, mouse and guinea pig cardiac muscle, *J. Ultrastruct. Research*, 1958, **1**, 271.

60 *a*. SJÖSTRAND, F. S., A new ultrastructural element of the membranes in mitochondria and of some cytoplasmic membranes, *J. Ultrastruct. Research*, 1963, **9**, 340.

61. STENGER, R. J., and SPIRO, D., The ultrastructure of mammalian cardiac muscle, *J. Biophysic. and Biochem. Cytol.*, 1961, **9**, 325.

61 *a*. STOECKENIUS, W., Some electronmicroscopical observations on liquid-crystalline phases in lipid-water systems, *J. Cell Biol.*, 1962, **12**, 221.

62. STUDNIČKA, F. K., Die Organisation der lebendigen Masse, *in* Handbuch der mikroskopischen Anatomie des Menschen, Berlin, Springer 1927, I/1, 421.
63. TAMARIN, A., and SREEBNY, L. M., An analysis of desmosome shape, size, and orientation by the use of histometric and densitometric methods with electron microscopy, *J. Cell Biol.*, 1963, **18**, 125.
64. TAUC, L., Neurophysiologie comparée, Interaction non synaptique entre deux neurones adjacents du ganglion abdominal de l'Aplysie, *Compt. rend. Acad. sc.*, 1959, **248**, 1857.
65. TSUBO, I., and BRANDT, P. W., An electron microscopic study of the Malpighian tubules

of the grasshopper, *Dissosteira carolina*, *J. Ultrastruct. Research*, 1962, **6**, 28.

66. TYLER, A., MONROY, A., KAO, C. Y., and GRUNDFEST, H., Membrane potential and resistance of the starfish egg before and after fertilization, *Biol. Bull.*, 1956, **111**, 153.
67. USSING, H. H., *Harvey Lectures*, 1963, in press.
68. VAN BREEMEN, V. L., Intercalated discs in heart muscle studied with the electron microscope, *Anat. Rec.*, 1953, **117**, 49.

68 *a*. VAN DER LOOS, H., Fine structure of synapses in the cerebral cortex, *Z. Zellforsch.*, 1963, **60**, 815.

69. WATANABE, A., and BULLOCK, T. H., Modulation of activity of one neuron by subthreshold slow potentials in another in lobster cardiac ganglion, *J. Gen. Physiol.*, 1960, **43**, 1031.
70. WATANABE, A., and GRUNDFEST, H., Impulse propagation at the septal and commissural junctions of crayfish lateral giant axons, *J. Gen. Physiol.*, 1961, **45**, 267.
71. WATANABE, A., and TAKEDA, K., The spread of excitation among neurons in the heart ganglion of the stomatopod, *Squilla oratoria*, *J. Gen. Physiol.*, 1963, **46**, 773.
72. WEIDMANN, S., Electrical characteristics of sepia axons, *J. Physiol.*, 1951, **114**, 372.

72 *a*. WEIDMAN, S., The electrical constants of Purkinje fibres, *J. Physiol.*, 1952, **118**, 348.

73. WIENER, J., SPIRO, D., and LOEWENSTEIN, W. R., Studies on an epithelial (gland) cell junction. II. Surface structure, *J. Cell Biol.*, **22**, 1964, 587.
74. WILSON, D. M., The connections between the lateral giant fibers of earthworms, *Comp. Biochem. and Physiol.*, 1961, **3**, 274.
75. WOOD, R. L., Intercellular attachment in the epithelium of hydra as revealed by electron microscopy, *J. Biophysic. and Biochem. Cytol.*, 1959, **6**, 343.

75 *a*. WOODBURY, J. W., and CRILL, W. E., *in* Nervous inhibition, (E. Florey, editor), New York, Pergamon Press, 1961.

76. ZETTERQVIST, H., The ultrastructural organization of the columnar absorbing cells of the mouse intestine, Stockholm, Aktiebolaget Godvil, 1956.